POLITECNICO MILANO 1863

SCUOLA DI INGEGNERIA INDUSTRIALE E DELL'INFORMAZIONE

Extended Abstract of the Thesis

An Automated CFD Workflow for Mating Gears Design Optimization

Laurea Magistrale in Aeronautical Engineering - Ingegneria Aeronautica

Author: Alessandro Tommasi, 10700642

Advisor: Prof. Federico Piscaglia

Co-advisor: Prof. Franco Concli

Academic year: 2024-2025

---

1. Introduction

The analysis of geared systems interacting with fluids, such as working fluids and lubricants, is a critical requirement in various engineering sectors, ranging from aerospace to petrochemical. Historically, the scientific community has relied on analytical formulations or lumped-parameter models due to their computational efficiency. However, these simplified approaches often fail to account for the complex three-dimensional coupling of physical mechanisms such as internal leakage, cavitation, and aeration. Although computational fluid dynamics (CFD) offers a robust framework to investigate these localized phenomena, simulating mating gears presents substantial challenges due to the continuous deformation of the internal fluid domain. The primary objective of this research is the development of a fully automated, high-fidelity CFD workflow. Unlike traditional approaches that require frequent user intervention or rely on non-conservative overlapping grids, the proposed routine enables a seamless transition from design parameters to final results without further manual operations, while preserving numerical accuracy. The key contribution introduced in this workflow is that it does not merely apply existing dynamic mesh techniques, but integrates geometry generation, mesh motion and topology change into a single automated and scalable framework, explicitly designed to remove the pre-processing complexity and serial bottlenecks that limit current high-fidelity CFD simulations of mating gears.

2. State of the art

The numerical investigation of geared systems has evolved from early analytical and semi-empirical models (e.g., Ohlendorf, Mauz, and ISO/TR 14179-1), which fit equations for power loss to experimental results but offer no insights into underlying physical mechanisms. Lumped-parameter models followed, discretizing the domain into coarse control volumes and replacing partial differential equations with ordinary differential equations to predict global quantities like volumetric efficiency. Within the CFD framework, strategies are divided into meshless (e.g., Smooth Particle Hydrodynamics) and mesh-based techniques. While meshless approaches avoid grid handling, they are often better suited for predicting lubricant flow patterns than precise flow field quantities. Mesh-based methods range from simple static meshes to advanced moving-mesh techniques. Among these, Overlapping Grids (Chimera) offer geometric flexibility but suffer from non-conservative interpolation. In this context, the present work builds upon the Global Remeshing Approach by explicitly addressing its two main limitations reported in the literature [3]: the high preprocessing effort required to generate multiple meshes, and the computational cost associated with non-optimized remapping strategies.

3. Methodology

3.1. Mesh generation

The entire numerical workflow is developed within the open-source CFD framework OpenFOAM, which provides the infrastructure for automated mesh generation, dynamic mesh motion, and topology changes. The mesh generation process is fully automated and begins with the parametric construction of the gear geometry starting from a limited set of design parameters. The profile of a single tooth is defined analytically using involute-based curves for the flanks and circular arcs for the tip and root regions, and subsequently discretized into a finite set of points. Exploiting the intrinsic periodicity of spur gears, the complete two-dimensional geometry is obtained by rigidly rotating the discretized tooth profile about the gear axis, resulting in a point cloud that accurately describes the full gear contour. The planar geometry is then extruded to generate the three-dimensional model and automatically converted into triangulated STL surfaces suitable for mesh generation. Prior to discretization, the gear geometries are uniformly scaled down by a small factor to avoid excessively fine cells in the vicinity of the contact region, where zero-clearance conditions would otherwise impose severe constraints on the mesh resolution. This modeling choice is consistent with the scope of the present analysis, which focuses on macroscopic flow phenomena rather than contact-scale effects. In addition, the relative position and initial angular orientation of the gears are initialized to ensure a correct tooth–slot engagement from the start of the simulation, thereby preserving geometric consistency throughout the meshing and motion process.

A structured hexahedral background mesh is created using *blockMesh* and serves as a robust support for subsequent refinement and deformation operations. Local refinement regions are introduced around the gears and within the expected engagement zone to adequately resolve small clearances and regions characterized by high velocity and pressure gradients. The final surface-conforming mesh is produced using *snappyHexMesh*, yielding a hexahedral-dominant grid that conforms to the complex gear geometry while maintaining acceptable quality metrics (Fig. 1).

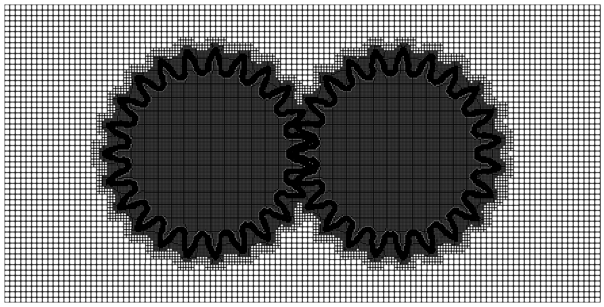

Figure 1: Gears mesh.

Owing to the geometric periodicity of the engagement process, only a limited sequence of meshes corresponding to different angular positions of the gears needs to be generated. This sequence is cyclically reused during the simulation, significantly reducing pre-processing complexity and computational overhead. Finally, grid independence is verified by means of a Grid Convergence Index (GCI) analysis based on Richardson extrapolation, providing a quantitative assessment of discretization-related uncertainty.

3.2. Dynamic mesh handling

The transient rotation of the gears is managed through a point-displacement boundary condition applied to the gear patches. The displacement is computed using the Rodrigues rotation formula, ensuring precise kinematic representation.

To maintain grid quality, a Laplace diffusion equation is solved for the cells. The diffusivity term is defined as directional to ensure a smooth propagation of deformations. Furthermore, the Space Conservation Law is enforced within the solver to account for volume changes due to boundary motion, preserving the conservation of mass.

3.3. Topology change

During the simulation, the continuous deformation induced by gear rotation lead to a progressive degradation of mesh quality. Before quality thresholds are exceeded, a topological mesh change is triggered and the computation is continued on an updated grid. This process is enabled through the *meshToMesh* utility, which provides a flexible framework for projecting solution fields from a source mesh to a target mesh while maintaining consistency across successive topological configurations.
Within this framework, different mapping strategies can be employed. By default, *meshToMesh* relies on an intersection-based method, which ensures conservative field transfer through the evaluation of geometric overlaps between source and target cells, albeit at a relatively high computational cost. To broaden the applicability of the methodology, the utility was extended to also support a nearest-neighbor interpolation scheme, in which source and target cells are associated based on spatial proximity. This alternative approach significantly reduces remapping time, at the expense of a less rigorous conservation of integral quantities. The choice between these strategies therefore reflects a trade-off between numerical accuracy and computational efficiency, depending on mesh similarity, resolution, and problem complexity.
Compared to earlier serial implementations, the adoption of *meshToMesh* allows the remapping stage to be fully parallelized, eliminating the major bottleneck associated with reconstructing and redistributing solution fields on a single processor. Additional performance improvements arise from optimized memory management, whereby the source mesh is retained in memory while the target mesh is loaded, avoiding redundant input/output operations and substantially reducing remapping overhead.
This strategy significantly reduces remapping overhead and removes the serial mapping stages typical of earlier workflows, making long transient simulations computationally affordable.

4. Validation

The numerical methodology is validated against experimental measurements available in the literature for a pair of spur gears operating under fully flooded and pressurized conditions. The experimental setup consists of two mating gears housed within a rigid casing filled with lubricant, where the driving gear is coupled to an electric motor while the driven gear rotates freely without transmitting load. The rotational speed is constant and the resistant torque acting on the system are measured, allowing the assessment of load-independent power losses associated with fluid–gear interaction. Additional experiments performed without the gears installed enable the isolation of bearing and seal losses, ensuring a consistent comparison with the numerical model.
The numerical simulations are carried out using a transient finite-volume CFD solver. The incompressible Navier–Stokes equations are solved under the laminar flow assumption, which is justified by the characteristic Reynolds numbers of the investigated operating conditions. The lubricant is modeled as a Newtonian fluid with constant physical properties, and the flow is assumed to be isothermal. To reduce computational cost, geometric symmetry is exploited, allowing the simulation of a reduced domain without significantly affecting solution accuracy.
Gear motion is prescribed through imposed boundary conditions. The simulations are initialized using a potential flow solution to enhance numerical robustness and convergence. Mechanical power losses are evaluated by computing the resisting torque acting on each gear, obtained from the integration of pressure and viscous forces over the gears surfaces.
Spatial discretization and mesh handling follow the automated procedure previously described, while temporal convergence is ensured by simulating multiple gear engagement cycles and time-averaging the solution over the final cycle. This approach enables a consistent and reliable comparison between numerical predictions and experimental data, providing validation of the proposed CFD workflow [1].

4.1. Results

Numerical simulations are performed at different rotational speeds, and convergence is achieved after two engagement cycles, with results time-averaged over the third cycle to ensure statistical robustness.
The predicted resisting torque shows excellent agreement with experimental data across the in-

vestigated operating range, accurately capturing both the magnitude and the trend of power losses as a function of rotational speed (Fig. 2). The comparison confirms the ability of the numerical model to reproduce the dominant fluid-dynamic mechanisms governing gear–lubricant interaction, despite the geometric simplifications introduced at the contact region.

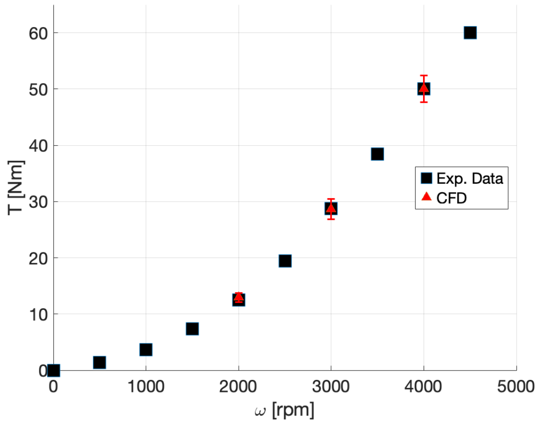

Figure 2: Experimental vs. numerical data.

Detailed analysis of the flow field reveals physically consistent pressure and velocity distributions. High-pressure regions develop on the leading flanks of the teeth, while low-pressure zones are observed on the trailing sides (Fig. 3), giving rise to characteristic secondary flows (Fig. 4).

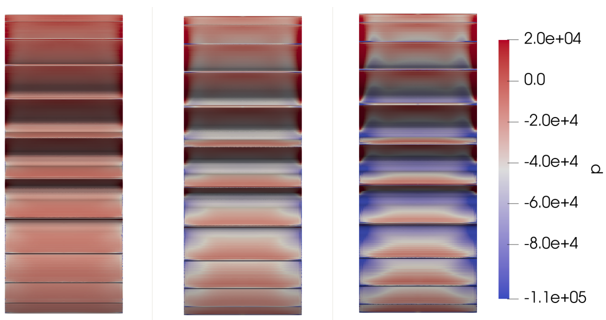

Figure 3: Relative pressure field: L) 2000rpm, C)3000rpm, R)4000rpm.

The simulations successfully reproduce well-known phenomena such as backflow at the onset of gear engagement (Fig. 5), pocketing effects associated with volume reduction between meshing teeth (Fig. 6), and centrifugal pressure gradients within the tooth cavities (Fig. 7).
The agreement is achieved without tuning model parameters against experimental data, confirming that the observed correspondence arises from the robustness of the mesh handling and motion strategy rather than from case-specific calibration.

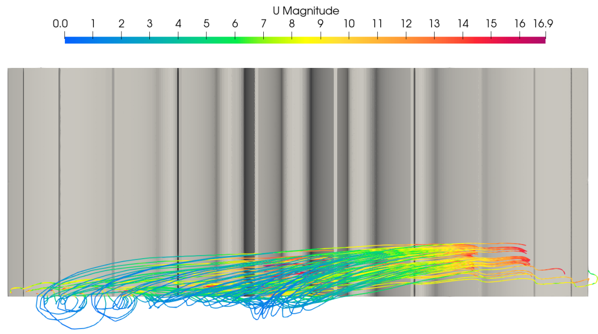

Figure 4: Streamlines, 3000rpm.

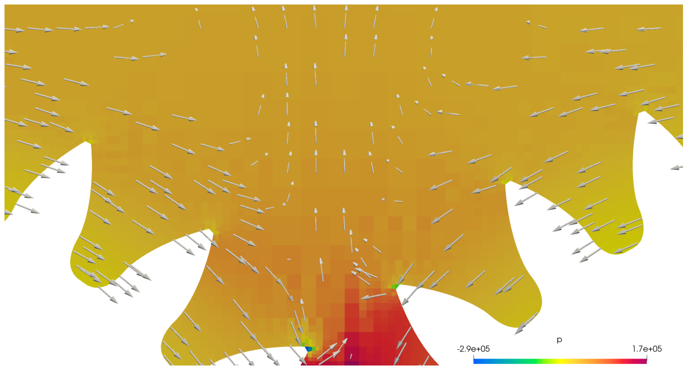

Figure 5: Backflow, 3000rpm.

5. Multi-phase

To assess the robustness and generality of the proposed workflow beyond single-phase conditions, the methodology is extended to multiphase simulations representative of realistic gearbox operating scenarios. In this configuration, oil and air are simultaneously modeled within the computational domain, with the casing partially filled to reproduce free-surface effects commonly encountered in gearboxes.
The multiphase flow is simulated using a Volume of Fluid (VoF) formulation within an incompressible framework. A single-fluid approach is adopted, in which the local physical properties are computed as weighted averages based on the phase volume fraction. Turbulence effects are accounted for through a Reynolds-averaged Navier–Stokes formulation adopting a $k-\epsilon$ turbulence model as closure of the system. Thermal effects are neglected under the isothermal assumption.
Two different lubricants (Oil 207 and Oil 208)

Oil	Aer_{exp}	$T_{exp}[Nm]$	$T_{CFD}[Nm]$	Δ_T
207	12.5%	0.12	0.1221	-1.8%
208	25%	0.125	0.1223	2.2%

Table 1: Aeration results

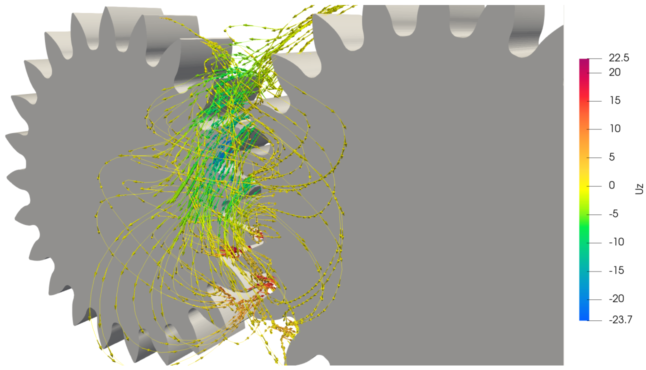

Figure 6: Pocketing, 3000rpm.

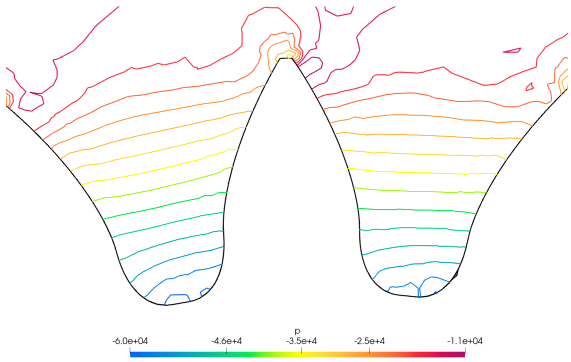

Figure 7: Relative pressure contours, 3000rpm.

are considered. They share the same density and viscosity but different surface tension, exhibiting different aeration behaviors, which constitute the focus of this section. Since air entrainment occurs at length scales that are typically smaller than the mesh resolution achievable in practical simulations, aeration is modeled through a sub-grid approach. In particular, Hirt's aeration model is employed, introducing a source term in the void-fraction transport equation to account for the balance between turbulence-induced air entrainment and stabilizing effects, given by gravity and surface tension [2]. The source is added in a cell if the turbulent contribution overcomes the stabilizing one.
The simulations capture, qualitatively and quantitatively (Tab. 1), air entrainment and transport within the gear cavities, confirming that the proposed framework can be robustly extended beyond single-phase [4].

6. Conclusions

This work presents a fully automated and flexible CFD workflow for the simulation of fluid–gear interaction in mating gear systems. The proposed methodology combines parametric geometry generation, automated mesh creation, dynamic mesh handling, and topology changes within a unified framework, significantly reducing user intervention during pre-processing stage while preserving geometric fidelity.
The integration of mesh morphing and mesh replacement strategies, enabled through the *meshToMesh* utility, allows accurate handling of large geometric deformations while maintaining acceptable mesh quality throughout the simulation. The parallelization of the remapping stage and the cyclic reuse of mesh sequences effectively remove key computational bottlenecks, making long transient simulations computationally affordable.
Validation against experimental data demonstrates that the developed approach accurately predicts load-independent power losses and reproduces the main flow features associated with mating gears, confirming the reliability of the numerical model despite the adopted geometric simplifications. The successful extension of the workflow to multiphase simulations further highlights its robustness and versatility, enabling the investigation of aeration phenomena under more realistic operating conditions.
While the present study focuses on isothermal and incompressible conditions, the modular structure of the workflow provides a solid basis for future extensions toward cavitation, thermal effects and more complex gear configurations, without requiring fundamental changes to the mesh handling strategy.

References

[1] F. Concli, A. Della Torre, C. Gorla, and G. Montenegro. A new integrated approach for the prediction of the load independent power losses of gears: Development of a mesh-handling algorithm to reduce the cfd simulation time. *Advances in Tribology*, page 8, 2016.

[2] C. W. Hirt. Modeling turbulent entrainment of air at a free surface. *Flow science, Inc.*, 2003.

[3] L. Maccioni and F. Concli. Computational fluid dynamics applied to lubricated mechanical components: Review of the approaches to simulate gears, bearings, and pumps. *Applied Sciences*, 10(24):8810, 12 2020.

[4] Mastrone M. N. and Concli F. Numerical modeling of fluid's aeration: Analysis of the power losses and lubricant distribution in gearboxes. *Journal of Applied and Computational Mechanics*, 9(1), 2023.